Sustainable Cities and Society 97 (2023) 104773

Contents lists available at ScienceDirect

Sustainable Cities and Society

journal homepage: www.elsevier.com/locate/scs

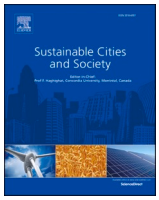

A simplified outdoor shading assessment method (OSAM) to identify outdoor shading requirements over the year within an urban context

Regwan Elrefai [a,b,*], Marialena Nikolopoulou [a]

[a] University of Kent, Kent School of Architecture and Planning, Canterbury, CT2 7NX, UK
[b] Cairo University, Architectural Engineering Department, Cairo, 12613, Egypt

ARTICLE INFO

Keywords:
Ladybug-tools
UTCI
Outdoor thermal comfort
Outdoor shading
Decision-support tool

ABSTRACT

This study proposes a novel way of using and presenting calculations of outdoor thermal comfort, to analyze the requirements of outdoor shading; by showing whether shading would be beneficial, harmful or ineffective – in a specified urban context – for every hour of the year. The simplified Outdoor Shading Assessment Method (OSAM) aims to assist in the early stages of outdoor shading analysis, acting as a decision-support tool regarding the type, application period, design and efficiency aspects of the shade required. The study uses the Universal Thermal Climate Index (UTCI) for thermal comfort evaluation, calculated through the Ladybug-tools (LBT 1.6). The method has been tested for the climate of Cairo against field measurements, revealing a strong correlation (R2 = 0.9267) for the UTCI. It also revealed potential overestimation in the Mean Radiant Temperature (MRT) simulation by newer versions of the LBT. Two climate examples, hot and temperate, are explored through two orientations and urban geometries, demonstrating varying outdoor shading requirements. For the E-W and N-S canyons (H/W = 1.3), Cairo's hot climate shows high shade benefit for at least 2 h per day for 171 and 250 days respectively, compared to 26 and 45 days for London's temperate climate.

1. Introduction

Studies to enhance the urban microclimate have been receiving more attention lately, especially in dense urban areas that have the biggest negative impacts from the downside of urbanization, such as pollution, greenery depletion, and increased ambient temperature due to the urban heat island (UHI) effect.

In hot climate areas, periods of heat discomfort can constitute a large portion of the year, playing a bigger role in impacting the quality of life. People cope with severe heat discomforts by relying on air-conditioned spaces, whether in buildings or vehicles, making the problem worse due to the added greenhouse gas emissions and anthropogenic heat. Not to mention the impact it has on the health and well-being of people (Vanos et al., 2010).

Open spaces in urban areas hold a great potential to improve people's quality of life, health and productivity (Elliott, Eon, & Breadsell, 2020). However, many of the public open areas lack the quality or design to be highly functional and utilized (Abbasi et al., 2016; Nasution & Zahrah, 2018). As has been highlighted in previous research, thermal comfort plays an important role in affecting the use of the outdoor spaces, regardless of the climate context (Elliott, Eon, & Breadsell, 2020; Givoni et al., 2003; Lai et al., 2014; Nikolopoulou & Lykoudis, 2007; Nikolopoulou et al., 2001). This research focuses on improving the comfort conditions outdoors, addressing one of the main factors that affect the microclimate in outdoor spaces, the direct solar radiation, by facilitating and supporting optimized outdoor shading applications (Lin et al., 2010; Pantavou et al., 2013).

1.1. Background

Thermal comfort, which is a condition of mind and is greatly subjective based on what a human feels in the thermal environment, is difficult to measure (ASHRAE 2004). It has been widely discussed in literature, in different fields of study, through a wide variety of approaches. Outdoor thermal comfort became more important with the increasing discussions on sustainable urban environments and significance of open spaces within the scope of climate change (Nikolopoulou, 2011).

With regard to urban environmental studies, the factors that affect thermal comfort can be classified into human-related; physiological, physical and psychological factors, and environmental factors; air temperature, humidity, wind and radiation (Nikolopoulou, 2011;

* Corresponding author.
E-mail address: rhme2@kent.ac.uk (R. Elrefai).

https://doi.org/10.1016/j.scs.2023.104773
Received 23 March 2023; Received in revised form 2 June 2023; Accepted 1 July 2023
Available online 4 July 2023

Nikolopoulou & Steemers, 2003). Various thermal comfort indices have been developed to determine thermal sensations in the environment, described in terms of neutral, hot or cold sensations with different ranges corresponding to each category, to identify the degree of discomfort (Copernicus Climate Change Service (C3S); Nikolopoulou, 2021). Some human-related factors, like clothing level and metabolic rate, are included, however, these theoretical based indices tend to ignore the impact of human physiological adaptation and psychology on their perceiving of comfort (Nikolopoulou, 2011; Zhao et al., 2021). Some survey-based studies have highlighted the significance of the human experiences and thermal adaptation on their feeling of comfort (e.g. (Lam, Hang, Zhang, Wang, & Ren, 2021; Nasir, Ahmad, & Ahmed, 2012; Nikolopoulou & Steemers, 2003).

The most common thermal comfort indices mentioned by Potchter et al. (2018) and Staiger, Laschewski, and Matzarakis (2019) include: The Standard Effective Temperature (SET), the Predicted Mean Vote (PMV) or the Perceived Temperature (PTJ) developed from it, the Physiologically Equivalent Temperature (PET), and the Universal Thermal Climate Index (UTCI). Both the PET and the UTCI have shown reliability, and unlike the SET and the PMV, were developed specifically for measuring thermal comfort in the outdoor environment (Fang, Feng, & Lin, 2017; Staiger, Laschewski, & Matzarakis, 2019). Moreover, they both use the unit of degree Celsius, facilitating their understanding and use by field practitioners, like designers and planners, who may not have deep knowledge in the meteorological field. Those are potentially the main reasons they are the most observed in literature for outdoor thermal comfort studies.

The PET and UTCI differ in the human heat-transfer model, but both are used to quantify the impact that air temperature, humidity, wind and radiation fluxes have on the human body (Matzarakis et al., 2016). The UTCI assumes self-adaptation regarding clothes and activity, which makes it suitable for the study of general population, rather than a specific group, which is different from the PET that requires inputs of clothing level and metabolic rate. The UTCI has shown validity for a great range of climates (Staiger, Laschewski, & Matzarakis, 2019), and when compared to PET in specific ones, it was reported more reliable. Studies in humid subtropical and temperate climates concluded that UTCI was more accurate than PET (Li, Liu, & Bao, 2022; Matzarakis et al., 2014). In addition, it was reported that the UTCI has higher sensitivity in responding to changes in temperature, humidity, solar radiation and wind, more like the human body response, while the PET relies more on air temperature (Blazejczyk et al., 2012). For those reasons, the UTCI is selected for use in the OSAM, which intends to be applied in a wide variety of climates by field practitioners.

"The UTCI is defined as the air temperature (T_a) of the reference condition causing the same model response as the actual condition"- [27, p. 94]. It is based on one of the most advanced multi-node thermophysiological models, the Fiala model. It requires inputs of air temperature, relative humidity, wind speed and radiation fluxes, which we calculate as Mean Radiant Temperature (MRT). MRT is defined as the uniform temperature an imaginary black enclosure would have that would allow equal amount of radiative heat exchange with a person inside it, as this person would get from a non-uniform real-life enclosure (ASHRAE 2001).

The MRT is greatly affected by the solar radiation in the outdoor environment. A person standing in an open space during the daytime would absorbs heat through incoming direct, sky diffused and reflected shortwave radiation. In addition, the incoming radiation increase the temperature of the surrounding surfaces, which then radiate heat back to the surrounding in the form of longwave radiation (Naboni et al., 2019). In dense urban areas, deep urban canyons trap the shortwave reflections through the increased surface area. This is aggravated by the artificial, high thermal emittance and capacity, materials, such as asphalt, which replace the natural grass and soil, causing an increase in the ambient temperature. Along with the wind being hindered in these environments, all these contribute to the UHI effect, where the temperatures in the urban areas are found higher than those in their neighboring rural areas (Oke, 1995).

Outdoor shading can alleviate UHI effects and provide thermal comfort (Peeters et al., 2020); it not only prevents direct solar radiation from falling on pedestrians, but also keeps the surrounding shaded surfaces at a lower temperature. Several studies highlighted the importance of shading. A study in the hot-arid climate of Cairo stated that shading can improve thermal comfort by up to 2.3 °C on the PET index scale (Mahgoub, 2015). Moreover, another study on urban shading by sun sails in the hot-dry summer of Cordoba, Spain (Garcia-Nevado, Beckers, & Coch, 2020), showed a decrease up to 16 °C in ground temperature and up to 6 °C in façade temperature due to the shades, while field surveys in Arizona also noted the effect of shades in enhancing pedestrian thermal comfort, with no difference reported in the perceived comfort due to the shade type (tree or solar canopy) in the hot-dry climate (Middel et al., 2016).

Outdoor shading can be provided through different ways: urban geometries, trees and artificial shading devices. Many studies on urban shading focus on the urban morphology and orientation aspects, which cannot be applied to existing urban areas but rather new ones (e.g. (Ali-Toudert & Mayer, 2006; Andreou, 2014)). Other studies focus on shading and cooling provided by trees, (e.g. (Kong et al., 2017; Wang, Wang, & Yang, 2018). However, there are limited studies and guidance on the process of identifying the outdoor shading requirements within an urban context; from, identifying the required shading periods, to efficiently locating the shade elements, and eventually increasing the overall efficiency of the shade application, especially on larger scales, such as shading an entire urban canyon. As Mackey et al. (2015) "… *there are virtually no agreed-upon methods currently available to assist in the design of outdoor shades to keep people comfortable.*"

With the recent and continuing advancements in simulation software, along with the understanding of the outdoor environment, they are increasingly employed in the built environment studies due to the benefits they have to offer, analyzing various alternative urban design proposals and their interaction with the climate, ahead of implementation. The development in data availability and computer speeds were an important factor (Mahgoub, 2015; Peeters et al., 2020). With an increasing interest amongst researchers on outdoor comfort studies, simulation software were encouraged to enhance their accuracy in the calculation of the outdoor comfort indices (Staiger, Laschewski, & Matzarakis, 2019).

There are several simulation software and packages available to simulate and analyze the outdoor thermal environment. However, they vary in their modeling of radiation, based on which the MRT is deduced (Naboni et al., 2019). The CFD software packages, based on advanced numerical techniques to simulate the fluid flow, heat transfer and other physical phenomena, are one of the most noted methods for simulating outdoor thermal comfort (Chung & Choo, 2011; Setaih et al., 2014). Some of the most observed simulation software that rely on CFD are: ENVI-met, Ladybug-Tools (LBT), ANSYS Fluent, Autodesk CFD and SOLWEIG. Other notable simulation software rely on different simplified methods and approaches for the simulation of the outdoor thermal comfort, like CitySim Pro and Rayman, however, they do not provide the level of detail as CFD software. More details on the different software and their simulations are found in literature (Jänicke, Meier, Hoelscher, & Scherer, 2015; Jänicke, Meier, Hoelscher, & Scherer, 2015; Pacifici & Nieto-Tolosa, 2021).

This study employs the new developing environmental simulation software, LBT, which are plug-ins of Grasshopper that runs within the Rhinoceros (Rhino) 3D modeling software. It utilizes its parametric aspect in providing rapid feedback on different designs and running dozens of simulations in a relatively short time, especially when CFD simulations are not included. This important advantage over other more accurate simulation software, such as ENVI-met, has contributed to its popularity, and made multiple simulations for the 8760 hours of the year that are required by the OSAM feasible. The LBT also has a user-friendly interface, facilitating its use by practitioners (Roudsari &

Pak, 2013). Not to mention it employs a variety of validated simulation engines, like Radiance, EnergyPlus and OpenFOAM, supporting its reliability and potential. These capabilities, along with the availability of pre-recorded weather data (through weather files), have opened the door to an enormous potential regarding assessing situations and designs before any real implementation takes place (Roudsari & Pak, 2013). The LBT have already been utilized in several optimization studies. A study on outdoor thermal comfort used LBT to simulate different street widths, orientations, and building heights to find the optimum (Ibrahim, Kershaw, Shepherd, & Elwy, 2021). Moreover, another study conducted daylight simulations to analyze and compare different daylighting louver systems for an office room (Eltaweel et al., 2020). In addition, the use of LBT was coupled with Ansys Fluent (fluid simulation software) to optimize green façades with regards to thermal comfort (Lin et al., 2023).

This study responds to the limited guidance and practical methods available to urban planners, designers and architects for effective outdoor shade applications, especially on large scales (e.g. street shading). The method proposed addresses the early analytical phase and facilitates decision-making regarding the design and application of shade. Currently, only one previous study has been found that employs the LBT to propose a workflow that supports/guides outdoor artificial shading devices application. The novel method "ComfortCover" proposed by Mackey et al. (2015) has played a role in guiding this research's proposed Outdoor Shading Assessment Method (OSAM); with similarities and differences highlighted in this paper.

1.2. Addition to current literature

A recent study in a hot-humid Mediterranean climate on outdoor shading of a similar scale (an urban canyon) (Peeters et al., 2020) used the Green Thermal Cluster Constant (Green CTTC) simulation model and the PET index to identify the minimum shading area required to provide thermal comfort within the canyon. However, the study lacked the spatial accuracy, with context shading not included, and the feasibility to perform the numerous amounts of simulations required to cover the entire year (Peeters et al., 2020).

The study by Mackey et al. (2015) was one of the first to introduce a simulation-based novel approach to optimize the application of an outdoor shading element, ComfortCover, developed from one of the existing shading methods for buildings, the 'Shaderade' (Mackey et al., 2015). The Shaderade and ComfortCover rely on hourly sun vectors projections, however, the ComfortCover substituted the building energy simulation of the Shaderade with the outdoor comfort index (UTCI). For the ComfortCover approach, the identification of a surface for the desired shade location and a position for the desired shading are required. Then, through the division of the shade surface into small cells, hourly calculations of the UTCI at the desired position are made, and deviations from the UTCI comfort range are summed up for the whole year for each cell. The outcome is then presented by coloring the cells blue or red, indicating shade will be beneficial or harmful respectively (Mackey et al., 2015).

The proposed Outdoor Shading Assessment (OSAM) method builds on the same concept of correlating between the hourly sun vectors projections and the UTCI values, as the ComfortCover method. However, instead of highlighting for the software user on the shade plane provided which parts would be overall beneficial or harmful based on the whole period of study, the OSAM provides the user with data regarding the shading requirements of the urban space for each hour of the year, presented in a chart divided into the 24 h of the day on one axis, and into the 365 days of the year on the other. Moreover, the OSAM incorporates a grid of points stretched over the study space, providing the data with respect to ratios of space; to facilitate the decision-making regarding large-scale applications, like the shading of a whole street.

Based on the previously mentioned data, OSAM addresses the gap in literature, by providing a relatively simple method that relies on new advanced technology, that can be used by urban planners, urban designers and architects, when approaching an outdoor shading assessment and/or design project of a large scale. OSAM builds on the concept of ComfortCover, but adjusts the LBT workflow and outcome representation, to provide a wider perspective on the shading requirements of a large-scale urban space for the entire year. It is intended as an assessment tool that can be used in the early analytical phase to guide the design and application of the shade, based on specific knowledge of the different seasonal requirements. Shade designs can target specific periods, based on sun path, for maximum benefit, while considering harm that can be done during other periods. In addition, decision-making can be facilitated through identified statistical data on shading requirements on the scale of a day or month or year.

2. Methodology

2.1. Simulation software

The proposed OSAM relies on workflow conducted through Rhino, Grasshopper and LBT (version 1.6) simulation software. The LBT plugins, Ladybug and Honeybee are used. The Ladybug is mainly used to import the EnergyPlus Weather (EPW) files, evaluate the solar access and provide a simplified calculation of the UTCI. While the Honeybee is incorporated for the more accurate simulation of the MRT through EnergyPlus and Radiance. More details are explained in the workflow section.

2.2. Thermal comfort index

As mentioned previously in the Introduction section, the proposed method (OSAM) relies on the UTCI to measure thermal comfort. It is calculated through the inputs of air temperature, relative humidity, wind speed and MRT (radiation fluxes).

The radiation fluxes that constitute the MRT, are either shortwave radiation (only during daytime), in the form of direct radiation from the sun, sky diffused radiation and radiation reflected on the surrounding surfaces, or longwave radiation radiated by the surrounding surfaces. Besides shortwave and longwave radiations calculations, other factors relating to the human perceiving them need to be identified, like body posture and orientation, and human outer surfaces emissivity and absorptivity (Naboni et al., 2019). Details on the UTCI calculation and the equations used can be referred to in literature (e.g. (Błażejczyk et al., 2010; Matzarakis et al., 2016; Naboni et al., 2019)).

The UTCI values are classified into ten categories, ranging from extreme heat stress to extreme cold stress, including neutral (no thermal stress). However, OSAM only uses the simple classification: hot, neutral and cold, where the neutral range is ($9 \leq \text{UTCI} < 26$), values below 9 are cold and above 26 are hot (Błażejczyk et al., 2010).

There are two approaches to simulating the UTCI through the LBT; by relying on the ladybug components, or incorporating the honeybee components along with the plugged-in simulation engines (EnergyPlus and Radiance). More on the simulation is discussed in the workflow section (2.4).

2.3. Theoretical case study

To present the use of the OSAM, a hypothetical urban canyon model is created on Rhino 7 software[1] (Figs. 1 and 2). The iron grid is chosen for simplicity, and two different Height-to-Width ratios are explored through changing the model's building heights only, to allow comparison of results. Firstly, the H/W ratio is set to 1.3, which is an approximate value for the H/W ratio analyzed for one of the canyons in a central

[1] Rhino 7 is currently the latest available version, and it is fully compatible with LBT 1.6 used in this study.

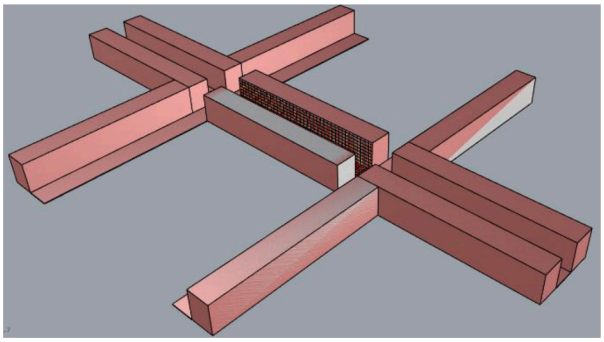

Fig. 1. A hypothetical urban canyon model used for the simulation of outdoor thermal comfort.

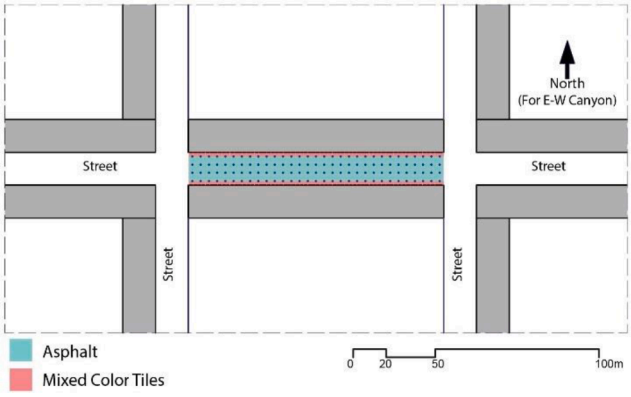

Fig. 2. Top view of the urban canyon showing the grid of points where UTCI measurements are made.

Fig. 3. Map showing part of the Mohandessin Area, observed for the H/W ratios (Google Earth 2023).

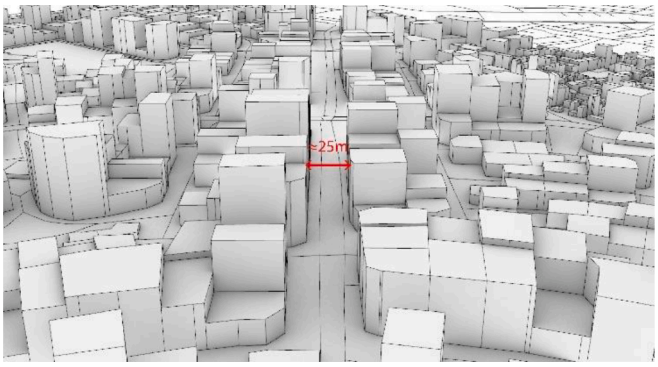

Fig. 4. Part of the 3D model for the same area in Mohandessin shown in Fig. 3, with the approximate width (25 m) indicated for the observed canyon (The Central Agency 2022).

district in the Greater Cairo in Egypt (Figs. 3 and 4), called the Mohandessin. This area was chosen for its limited public open spaces, which are mainly observed in the form of urban canyons that withhold the streets network. Enhancing the microclimate within the canyons can encourage their partial or full pedestrianization for the public benefit. Secondly, to test OSAM for varying geometries, the buildings heights in the model were lowered to provide a H/W ratio equal to 0.9, reflecting a less dense urban area.

The modeled urban canyons' heights are 26 m for (H/W = 1.3) and 18 m for (H/W = 0.9), while the width is fixed at 20 m. The length is set to be six times the height of buildings (156 m based on the taller buildings), to identify as an urban canyon (Oke, 1988).

Firstly, the model with (H/W = 1.3) is studied for two different orientations, parallel to the North-South (N-S) and East-West (E-W). Each orientation is analyzed for two different climates, using two different weather files: Cairo 623,660 (IWEC) and London Gatwick 037760 (IWEC), both obtained from the U.S. Department of Energy's website (ASHRAE 2001; DOE 2023). Then, the lower H/W ratio (0.9) is tested for the N-S orientation for both climates and the results are compared. These comparisons are essential to evaluate the potential of the method in different conditions. Investigating the impact of different orientations, geometries and climates on the outcomes of the OSAM, enables us to evaluate the impact on the decision-making process regarding shading application.

Cairo (30°06′ N 31°2′E) is the capital city of Egypt with climate classified as hot desert climate (BWh) according to the Köppen-Geiger Climate Classification. It is characterized by hot dry summers and moderate winters, with very little rainfall. Based on the weather file used in this study (Cairo 623,660 IWEC), the annual average air temperature is ~ 22 °C, with the minimum being 7 °C and the maximum 43 °C. London (51°.51′N -0°12′E) is the capital city of the United Kingdom, with a temperate oceanic climate (Cfb). It is characterized by cool winters and warm summers, with a significant amount of rainfall during the year. Based on the weather file used in this study (London Gatwick 037760 IWEC), the annual average air temperature is ~ 6 °C, with minimum being ~ -6 °C and the maximum ~ 31 °C.

2.4. Workflow

The correlation between the hourly sun vectors projections and the UTCI measurements in the ComfortCover method, constitute the base of the OSAM. However, for the OSAM, the UTCI is calculated at several positions instead of one. A 5-meter spacing grid is used in the canyon, with a total of 124 points where direct solar exposure is assessed for the calculation of the UTCI, at a height of 1.1 m.

Moreover, no shade surface is proposed, but instead analysis is conducted for the shading required at the different positions on the grid. Furthermore, instead of using the UTCI values and calculating the deviation from the comfort range, the UTCI values are then classified into three basic categories (referred to as UTCI Conditions): 0 if comfortable, -1 if unacceptably cold and +1 if unacceptably hot. In addition, the UTCI conditions are not summed up for all the hours of the year, but instead they are summed up for all the positions for each hour of the year, and each hour is presented separately. As the OSAM accounts for the surrounding urban context to the study area, shading by the buildings is considered, and if a position where calculations are made is shaded by the context at any hour of the year, the UTCI calculated for that position for that hour is replaced by the value 0. This is done to avoid including values of positions already shaded by the context in the shading requirement analysis.

As the UTCI can be simulated through two different methods in the LBT; using Ladybug or Honeybee plugins, the more accurate UTCI

through Honeybee is used, however, the outcome of the Ladybug workflow is presented in the Appendix (Fig. 12). The main differences between the two methods lie in the simulation of the MRT. Honeybee incorporates surface temperatures simulated through EnergyPlus, with their surface view factors obtained by Radiance in calculating the longwave MRT, unlike Ladybug's solar outdoor MRT where the user assumes that surface temperatures are equal to air temperatures. Moreover, Radiance in Honeybee also includes shortwave solar reflections on the surrounding surfaces, whereas in Ladybug only ground reflection is estimated. Hence, it is important to note that when UTCI is calculated through the Ladybug plugins, there will be no difference between the UTCI values at the different positions for the same hour of the year, but the exposure of a standing person at the defined positions to direct solar radiation will be different as shaded by the context. Contrarily, for UTCI simulations through the Honeybee components, the UTCI values will differ for the various positions, for the same hour of the year.

For the simulation of UTCI through Honeybee plugins, additional detailing for the model is required, along with the identification of some parameters. Firstly, the model surfaces were divided on a grid, as each surface unit will have a uniform simulated surface temperature; hence smaller surface units will increase simulation accuracy but will require more simulation time. For the presented case studies, and based on the validation study performed, it was found adequate to divide the ground surface on a 2.5 × 2.5 m grid, while the canyon building façades were divided on a 3 × 4 m grid. Secondly, the construction of the urban canyon was customized based on the case study used for validating the simulation workflow, which are an adequate reflection of constructions in the Greater Cairo, Egypt. Glazing ratio was defined as 20% of walls and were assigned the default construction of 'Generic Clear Glass'. Table 1 shows some properties of the main constructions used.

The Radiance parameters were adjusted to achieve reliable simulation outcomes for the studied model. The highest quality level was selected from the component defaults for the "rfluxmtx | annual" recipe type. However, the 'direct thresholding' parameter was changed to 0.05 instead of 0.15 based on the recommendations for highest accuracy by Radiance (2023), and the "Ambient Bounces" were changed to 1 instead of 6, as it was found to produce the least differences from the field measurements in MRT during the hours of direct solar exposure.

No CFD simulations were performed, as they would require a significant amount of time, which would be a major constraint and unfeasible for performing the 981,120 calculations in the case study. The target areas studied are in a dense urban environment where wind is hindered, and its effect on the UTCI outcome is low (Natanian, Kastner, Dogan, & Auer, 2020; Pacifici & Nieto-Tolosa, 2021). As a result, Eq. (1), based on the wind power law equation, is used for adjusting the wind values from the 10-meter-high weather station values to the 2-meter--high pedestrian level values, while also accounting for the different terrain types (ASHRAE 2005; Aynsley et al., 1977; Tahbaz, 2016). The equation has been re-arranged and different symbols were used, as defined below.

$$V_Z = V_{met} * \frac{\left[\frac{H_z}{G_z}\right]^{\alpha}}{\left[\frac{H_{met}}{G_{met}}\right]^{\alpha_{met}}} \quad (1)$$

Where V_z is the wind velocity (m/s) at the wanted location (Z), which is calculated from the weather file value, V_{met} is the wind speed (m/s) from the meteorological station file (at a 10-meter height), H_z is the height (m) at the wanted location (which is at a 2-meter height for pedestrian level), H_{met} is the meteorological station measurement height (m) (10 meters in most cases), and G_z and G_{met} are the wind boundary layer thickness (m) for the wanted location and the meteorological station respectively. The wind boundary thickness layer (G) and exponent (α) are obtained from Table 2 based on the terrain types. For the meteorological station, the typical values used are those of terrain category 3, $G_{met} = 270$ m and $\alpha_{met} = 0.14$, while the values used for the wanted design location will be selected from terrain category 1, $G_{met} = 460$ m and $\alpha_{met} = 0.33$, as the study targets dense urban areas.

Fig. 5 shows a flowchart that explains the algorithm taking place after obtaining the UTCI results from either component, i.e. the Ladybug or the Honeybee component, and presenting them in an excel sheet for the graphical representation of the results. For the theoretical case study presented, we have the UTCI values for 124 positions multiplied by 8760 hours of the year for each point, providing a total of 1086,240 results. To simplify the presentation of the UTCI values, the UTCI conditions are used instead, which classifies and replaces the initial values by 0, -1 or +1 for comfortable, unacceptably cold or unacceptably hot respectively. Then, the exposure to direct solar radiation for each position (at a height of 1.1 meters) for each hour of the year is checked, and the UTCI condition for non-exposed/ shaded positions are then changed to 0.

The values obtained after this point, if negative (showing unacceptable cold sensation), means shading this position will be harmful, and if positive (showing unacceptable hot sensation), means shading will be beneficial. Summation for values of all positions calculated at the same hour of the year is performed; a maximum value of 124 indicates that all positions are exposed to direct solar radiation at that hour and are unacceptably hot (shading the space is beneficial), while a minimum value of -124 indicates that all positions are exposed to direct solar radiation at that hour and are unacceptably cold (shading the space is harmful), with a range of values being in between the two. A value of 0 means that either none of the positions have direct solar exposure or they are exposed but with comfortable sensation, so shading in this case is not required and will be ineffective. The results are presented in an excel sheet, with the columns divided into the 24 h of the day, and the rows divided into the 365 days of the year. Hence, each cell on the graph will be the value obtained from all the positions for a specific single hour of the year.

Table 1
Construction properties used for the honeybee model simulations.

	Wall	Roof	Ground
Solar reflectivity	60% (light color)	60% (light color)	Asphalt 13% (default) Tiles 50% (mix colored tiles)
Thermal resistance (m^2.K/W)	0.43	2.12	Asphalt 0.25 (default) Tiles 0.41

Table 2
Recommended parameters (α and G values) for different terrain types (ASHRAE 2005).

Terrain category	Description	Exponent (α)	Layer thickness (G), m
1	Large city centers, in which at least 50% of buildings are higher than 21.3 m, over a distance of at least 0.8 km or 10 times the height of the structure upwind, whichever is greater	0.33	460
2	Urban and suburban areas, wooded areas, or other terrain with numerous closely spaced obstructions having the size of single-family dwellings or larger, over a distance of at least 460 m or 10 times the height of the structure upwind, whichever is greater	0.22	370
3	Open terrain with scattered obstructions having heights generally less than 9.1 m, including flat open country typical of meteorological station surroundings	0.14	270
4	Flat, unobstructed areas exposed to wind flowing over water for at least 1.6 km, over a distance of 460 m or 10 times the height of the structure inland, whichever is greater	0.10	210

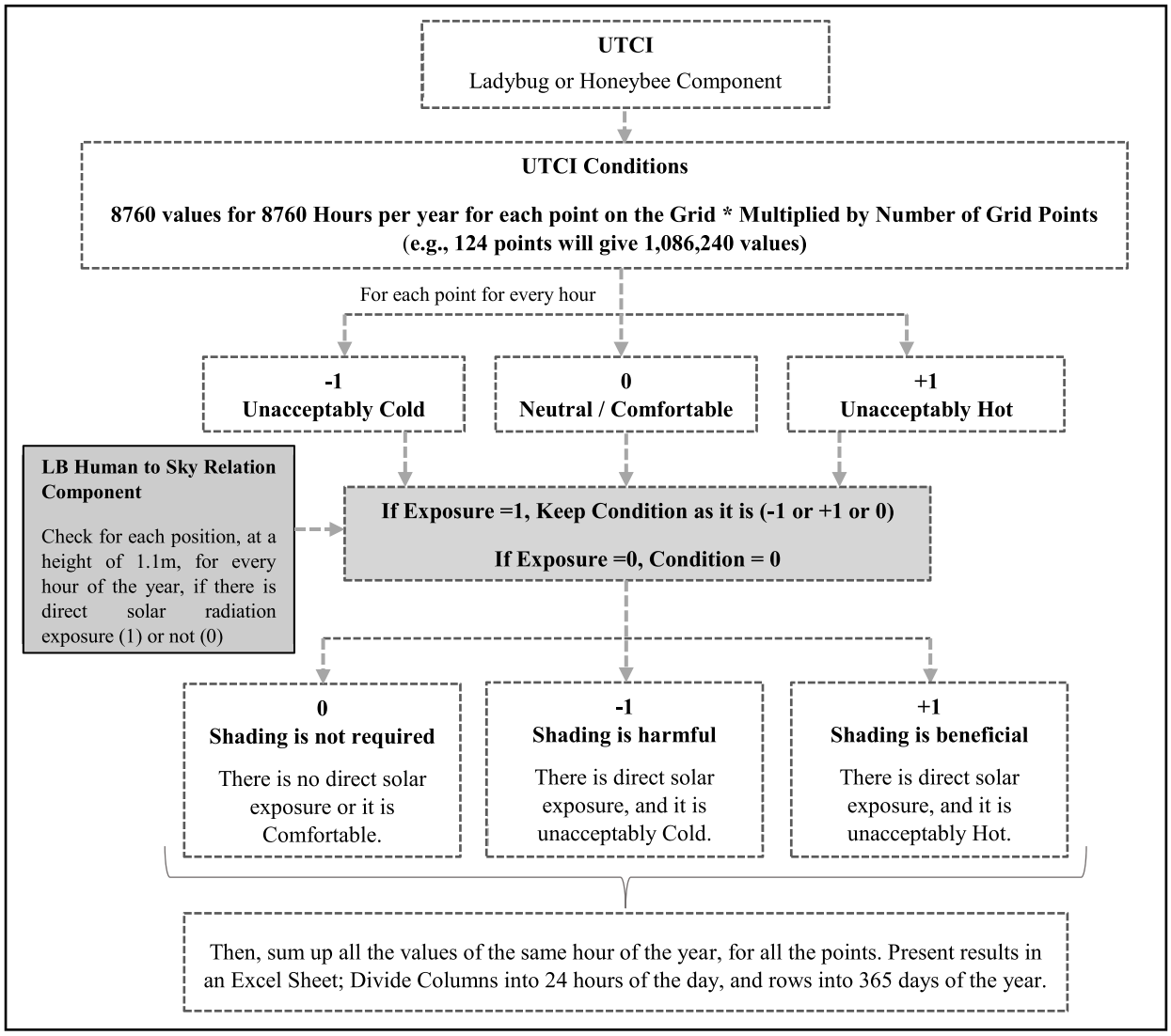

Fig. 5. A flowchart explaining the steps after obtaining the results from the UTCI component (whether it is the ladybug or honeybee component) and presenting them in an excel sheet.

To simplify the reading of the resulted graphs, a color key is defined where a color is given for each specified range of results, and it is presented in Fig. 9 in Section 3. As mentioned earlier, values from 1 to 124 indicate shading will be beneficial, while values from -1 to -124 indicate shading will be harmful. However, to evaluate the effectiveness of the shade application, it is useful to know the extent to which the space shading will be beneficial or harmful. Hence, the color key divides the positive values in the middle into two groups: 1 to 61 and 62 to 124, as well as the negative values into groups -1 to -61 and -62 to-124. This proposed division allows the easy identification of the percentage of positions that have a certain shading requirement, if they are less or more than 50% of the positions spread over the space considered. So, for example, a value of 45 in the proposed case indicates that less than 50% of the positions studied (total of 124 positions) will benefit from shading, meaning approximately less than 50% of the space area. Hence, decisions about shading the entire space can be made, especially when the requirements of all the hours of the year can be seen all together, arranged by days and months.

2.5. Simulation validation

Various previous studies have used the LBT simulation to calculate the UTCI, where the results have shown reliability, either against the validated ENVI-met software results or compared to field measurements (e.g. (Evola et al., 2020; Ibrahim, Kershaw, Shepherd, & Elwy, 2021, 2020; Xu et al., 2019)).

To validate the current workflow, the study site and field measurements from an urban canyon in a university campus in Cairo are used (Elwy & Ibrahim, 2022), which had been used by a previous study to validate the UTCI results obtained by the LBT (Legacy version 0.0.69) – Honeybee components (Ibrahim, Kershaw, Shepherd, & Elwy, 2021), to validate the UTCI calculated through the LBT (version 1.6), using both Ladybug and Honeybee plugins. The site model, shown in Fig. 6, was developed based on data provided by Elwy and Ibrahim (2022) and personal observation of the site.

The field measurements took place on 6th August 2017 between the hours 07:00 and 19:00 (Elwy & Ibrahim, 2022). The equipment, presented in Table 3, included the Onset HOBO-U30 weather station, which was used for the dry-bulb temperature, wind speed and relative humidity measurements, while the black globe temperature was obtained using the Extech HT30 Heat Stress WBGT meter.

Ibrahim, Kershaw, Shepherd, and Elwy (2021) validated the Cairo weather file (IWEC), which is used in this paper for both the validation and OSAM application, against field measurements and highlighted its reliability for further use. Moreover, their study used a ladybug component based on the wind power law for simple adjustment of wind

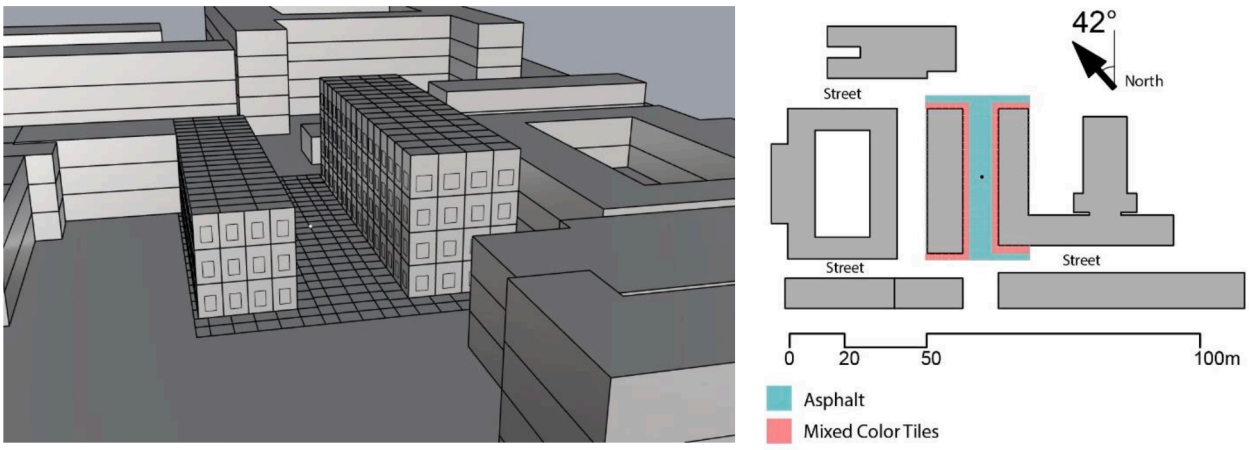

Fig. 6. A perspective view (left) and top view (right) of the field measurements' site model on Rhino software, with the position of measurements marked by a point in the middle. Model built by Author based on data obtained from Elwy and Ibrahim (2022) and personal observations.

Table 3
The range and accuracy of the sensors used in field measurements (Elwy & Ibrahim, 2022).

Sensor	Parameter measured	Range	Accuracy
S-THB-M002	Dry-Bulb Temperature	−40 to 75 °C	± 0.21 °C (at 0 – 50 °C)
S-THB-M002	Relative Humidity	0 to 100%	± 2.5% (at 10 – 90%)
S-WSB-M003	Wind Speed	0 to 76 m/s	± 1.1 m/s or 4% of reading
HT30	Black Globe Temperature	0 to 80 °C	± 3 °C (Outdoors)

values from the 10-meter-height at the weather station to the 2-meter--height pedestrian level in urban areas. However, as the component is no longer available in LBT (version 1.6), Eq. (1) is used instead. Furthermore, the same methods for calculating the MRT and UTCI from the field measurements used by Ibrahim, Kershaw, Shepherd, and Elwy (2021) were adopted in the current study. The field measurements MRT was calculated based on Eq. (2) (British Standards Institution, Ergonomics of the thermal environment 2001), while the MRT through ladybug was calculated through the ladybug *outdoor solar MRT* component, with surface temperatures assumed to be equal to air temperatures and ground reflectivity of value 0.26, based on the ratios of the materials present on the site and using the outcome of the default reflectivity value of asphalt and an assumed reflectivity of 50% for the red and beige cement tiles pavement.[2] The UTCI for the field measurements was calculated using the ladybug UTCI component and inserting the MRT values calculated earlier using Eq. (2), along with the wind, air temperature and relative humidity measured on site. Note that the wind speed values, obtained from field measurements and Eq. (1), were multiplied by 1.5 (factor used) before being input into any of the ladybug UTCI or the honeybee UTCI components, as those are ground level values, and the components requires wind speeds at the 10-meter--height meteorological station values.

$$MRT = \sqrt[4]{(T_g + 273)^4 + \frac{1.1 * 10^8 * v^{0.6}}{\varepsilon_g * D^{0.4}} * (T_g - T_a)} - 273. \quad (2)$$

Where T_g is the black globe temperature (°C), T_a is air temperature (°C), v is the wind speed (m/s), ε_g is the globe emissivity ($\varepsilon_g = 0.95$) and D is the diameter (D = 0.04 m) (Ibrahim, Kershaw, Shepherd, & Elwy, 2021).

Comparisons between the MRT and UTCI values for the on-site measurements, the ladybug components and the honeybee components are shown in Fig. 7, with the coefficient of determination (R^2) values shown in Fig. 8. The maximum difference from the field measurements in the MRT observed is 8.36 °C for ladybug and 16.63 °C for honeybee, compared to 8.01 °C obtained by Ibrahim, Kershaw, Shepherd, and Elwy (2021), while the maximum UTCI difference is 4.32 °C for ladybug and 2.22 °C for honeybee, compared to ~3.5 °C obtained

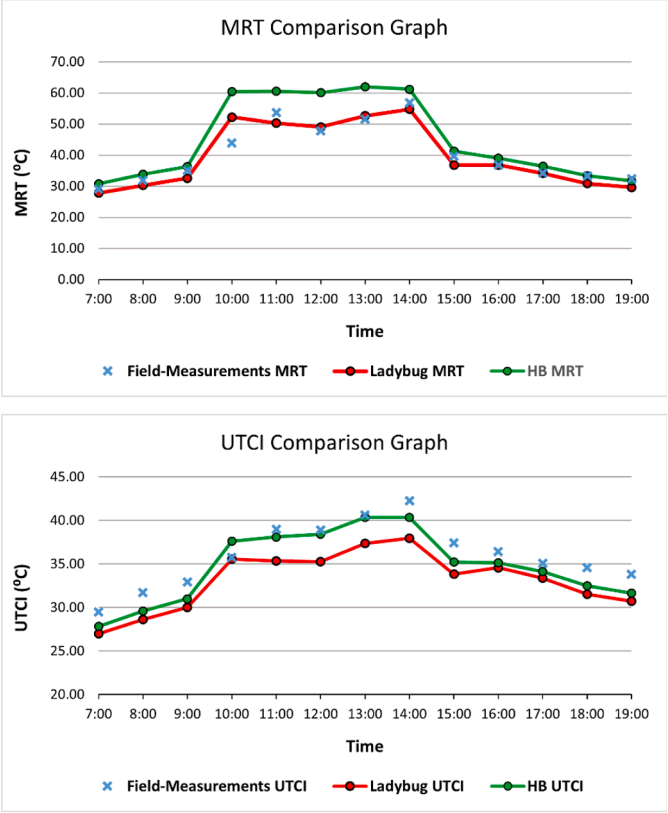

Fig. 7. Graphs showing the relationship between the values obtained from field-measurements and the values produced by ladybug and honeybee components for MRT (top row) and UTCI (bottom row).

[2] Solar reflectivity and percentage of total area are 0.5 and 35.5% for red and beige cement tiles pavement, and 0.13 and 64.5% for asphalt, respectively.

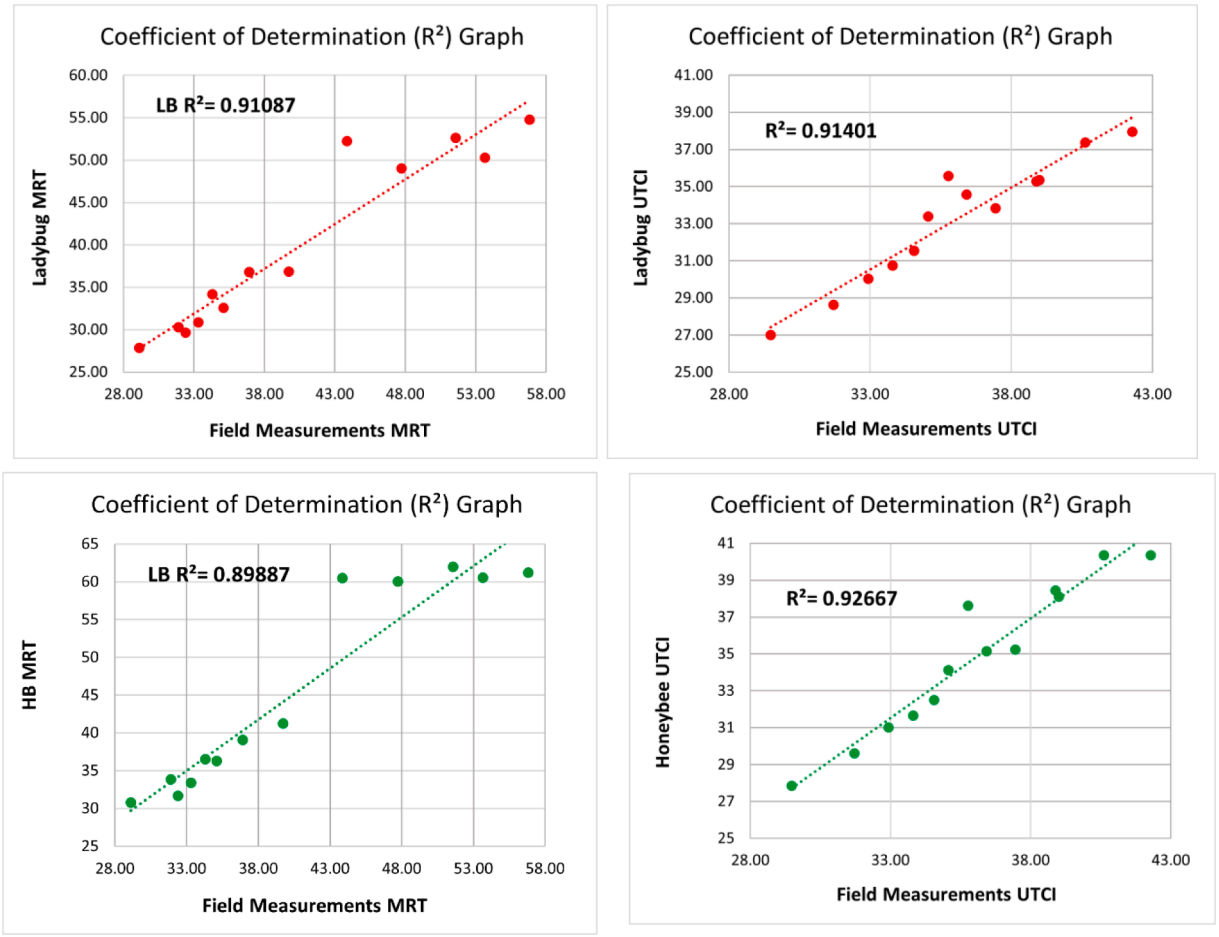

Fig. 8. Graphs showing the coefficient of detemination (R^2) for the MRT values (left) and UTCI values (right), obtained by the ladybug components (top row) and the honeybee components (bottom row), against field measurements outcome.

by Ibrahim, Kershaw, Shepherd, and Elwy (2021). Moreover, the ladybug values show a stronger correlation with the field measurement for the MRT (R^2 = 0.91087) compared to the honeybee values (R^2 = 0.89887), while for the UTCI, the honeybee values show a stronger correlation (R^2 = 0.92667) compared to ladybug (R^2 = 0.91401). The obtained correlation values are close to those obtained by Ibrahim, Kershaw, Shepherd, and Elwy (2021), which show R^2 = 0.9055 and R^2 = 0.9144 for MRT and UTCI respectively.

The large differences in the MRT between the honeybee and the field measurements outcomes are observed between the hours 10:00 and 14:00, which is when the position of simulation and measurements is exposed to direct solar radiation. This suggests that there might be an overestimation, in the shortwave solar radiation, simulated by Radiance. Moreover, the highest MRT difference was seen at 10 am, in both the results obtained by ladybug and honeybee, as well as those obtained by Ibrahim, Kershaw, Shepherd, and Elwy (2021) using LBT legacy version 0.0.69; which their study suggested might be due to the spatial resolution of the model, the global horizontal radiation from the weather file or the thermal admittance of the ground. However, the rest of the MRT results during direct solar exposure obtained by honeybee (LBT version 1.6), are still high compared to the field measurements outcome (up to 12.31 °C). One potential reason for the high difference can be attributed to the fact that in the newer versions of LBT, the solar radiation reflected on surrounding façades and falling on a person are accounted for using Radiance, mimicking the real environment. Moreover, the study by Evola et al. (2020) has noted that their simulation workflow on LBT, which did not account for solar radiation falling on a person from façade reflections, was more reliable against their field measurements in shaded areas, whereas in sunlit areas, it tends to overestimate it (by up to 6.1 °C). Their study also mentioned that ground surface temperatures in sunlit areas were also overestimated in the simulation (by around 4 °C).

Unlike the MRT results, the UTCI outcome of honeybee (LBT 1.6) showed the lowest variation from field measurements (2.22 °C) and the highest correlation (R^2 = 0.92667) compared to ladybug outcome and honeybee outcome (legacy version) by Ibrahim, Kershaw, Shepherd, and Elwy (2021). And since the shading assessment method presented (OSAM) merely relies on the UTCI, the workflow of honeybee (LBT 1.6) is sufficient for use.

However, it is important to note that, despite the simplicity with which the UTCI values were obtained through the Ladybug component, compared to those through Honeybee, the results indicate a good reliability, and can be used for the OSAM. However, further studies on its reliability in more complex contexts is suggested, since the Ladybug components do not incorporate the urban morphology, other than accounting for direct solar exposure, in the UTCI calculation.

3. Results

The OSAM methodology is tested through application in two different climatic contexts, Cairo and London, and for different geometries, through two different orientations, E-W and N-S, and H/W ratios (0.9 and 1.3). Firstly, the results of (H/W = 1.3) are presented; the outcomes of the workflow previously shown in Fig. 5 for each of the orientations, for the two climates, are shown in Fig. 9. The Color key for the classification of values in the graphs is shown in Fig. 9(A); Light red

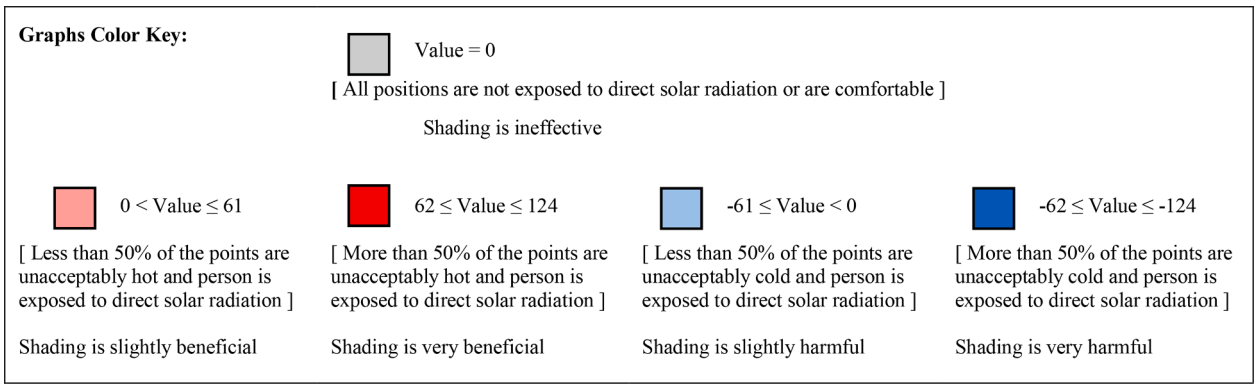

(A)

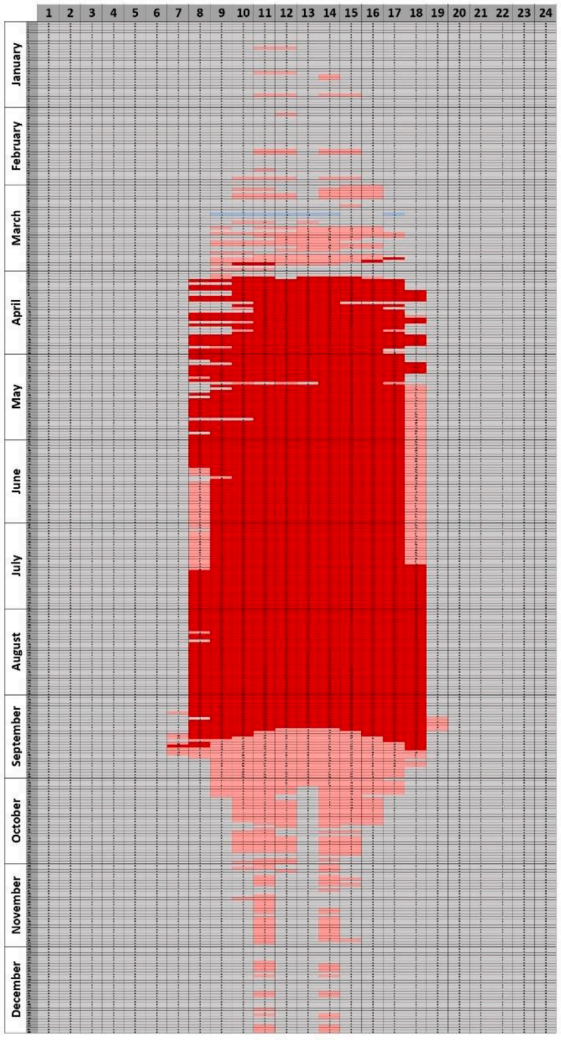

Cairo E-W Canyon (H/W = 1.3)

(B)

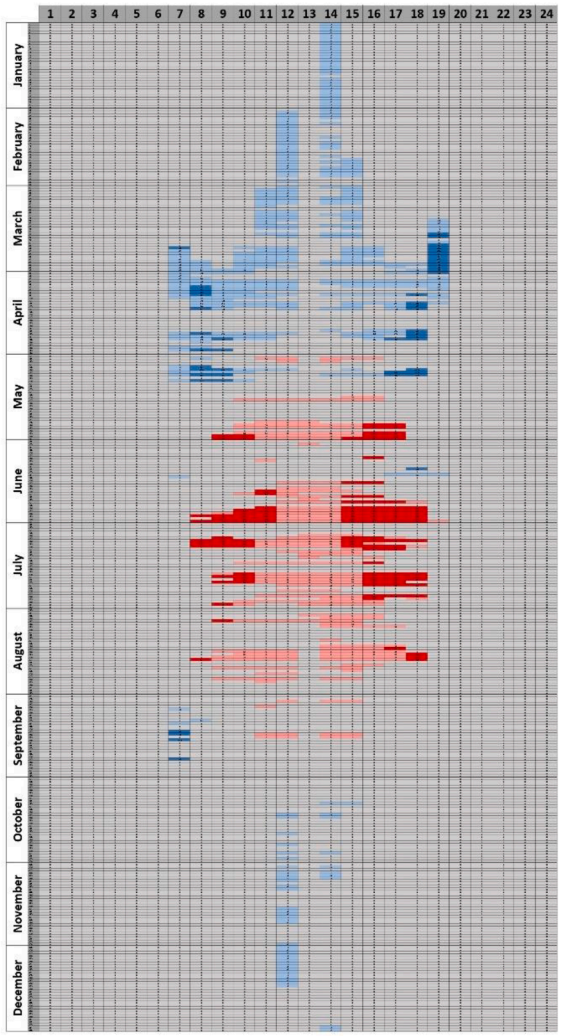

London E-W Canyon (H/W = 1.3)

(C)

Fig. 9. Shows the honeybee outcome of the UTCI conditions summed up for all grid points for all the hours of the year, with the columns being the 24 hours of the day, and the rows being 365 days of the year, for two different weather files (for canyon H/W = 1.3). (A) shows the graph's color key. (B) and (D) show results for Cairo's International Airport Weather File, while (C) and (E) are for London Gatwick's Weather File. (B) and (C) show the results of the E-W Oriented Urban Canyon, and (D) and (E) show those of the N-S Oriented Urban Canyon.

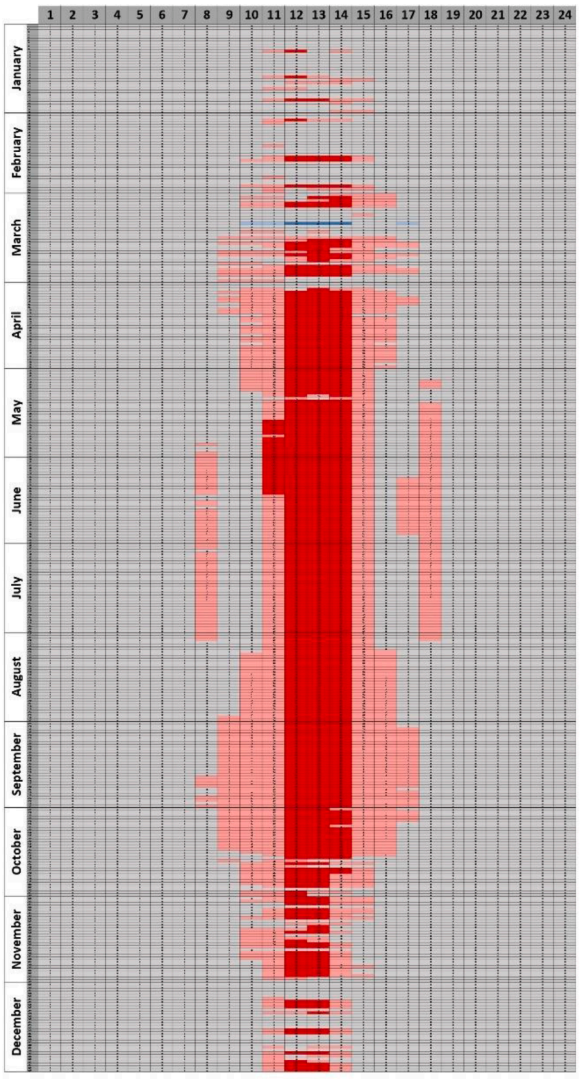

Cairo N-S Canyon (H/W = 1.3)

(D)

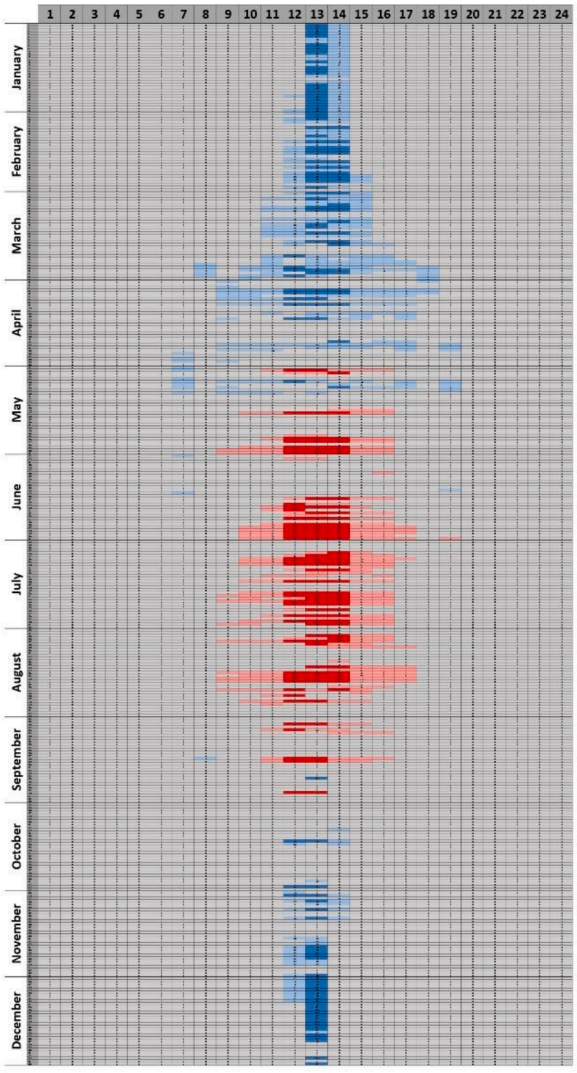

London N-S Canyon (H/W = 1.3)

(E)

Fig. 9. (*continued*).

color indicate low shade benefit (less than 50% of study positions require shade); Dark red color indicate high shade benefit (50% or more of study positions require shade); Light blue color indicate low shade harm (less than 50% of positions are harmed by shade); And dark blue color indicate high shade harm (more than 50% of study positions are harmed by shade).

The results of Cairo's weather file, Fig. 9(B & D), show periods were shading application can be beneficial for the presented urban context (dark red and light red cells), while periods where shading can be harmful are negligible (dark blue and light blue). To be more specific, for the E-W oriented urban canyon shown in Fig. 9(B), the majority of hours with high shade benefit (dark red) extend between beginning of April and around mid-September, mostly from 8 or 9 am to 5 or 6 pm, while periods with low shade benefit are seen diminishing through end of September to December, and in March.

On the other hand, for the same oriented canyon (E-W) for London Gatwick's weather file shown in Fig. 9(C), periods where shading can be beneficial are seen more segregated, through the months May to August. Low shade benefit periods are mainly within the same months during mid-day.

The N-S oriented urban canyons for both weather files shown in Fig. 9(D & E) show some differences from (B & C), respectively. For Cairo's N-S canyon, the high shade benefit periods expand over less hours of the day, with the majority from 12 noon to 2 pm. However, they extend for longer months, mainly starting towards the end of February and till the end of December. While for London's N-S oriented canyon, the high shade harm hours have increased, observed mainly from November till the first half of April, but only expand for around 1 to 3 h per day. The differences in the N-S oriented canyons from the E-W ones are understandable due to shading by the buildings in the early and late hours of the daytime, and having more direct solar exposure for the lower winter sun.

The pie charts in Fig. 10 show the percentages that each category of values constitute from the whole year for all graphs presented in Fig. 9. Cairo has a higher requirement for outdoor shading throughout the year, with 18.7% and 8.5% high shade benefit hours for E-W and N-S oriented canyons respectively, compared to 1.4% for both orientations of London. Table 4 shows some statistics obtained from the graphs for shade benefit/harm in terms of hours per day and days per year. The number of days per year with 2 or more high shade benefit hours for the E-W and N-S canyons for Cairo are 171 and 250 days, respectively, compared to 26 and 45 days for London. On the other hand, the number of days with 2 or

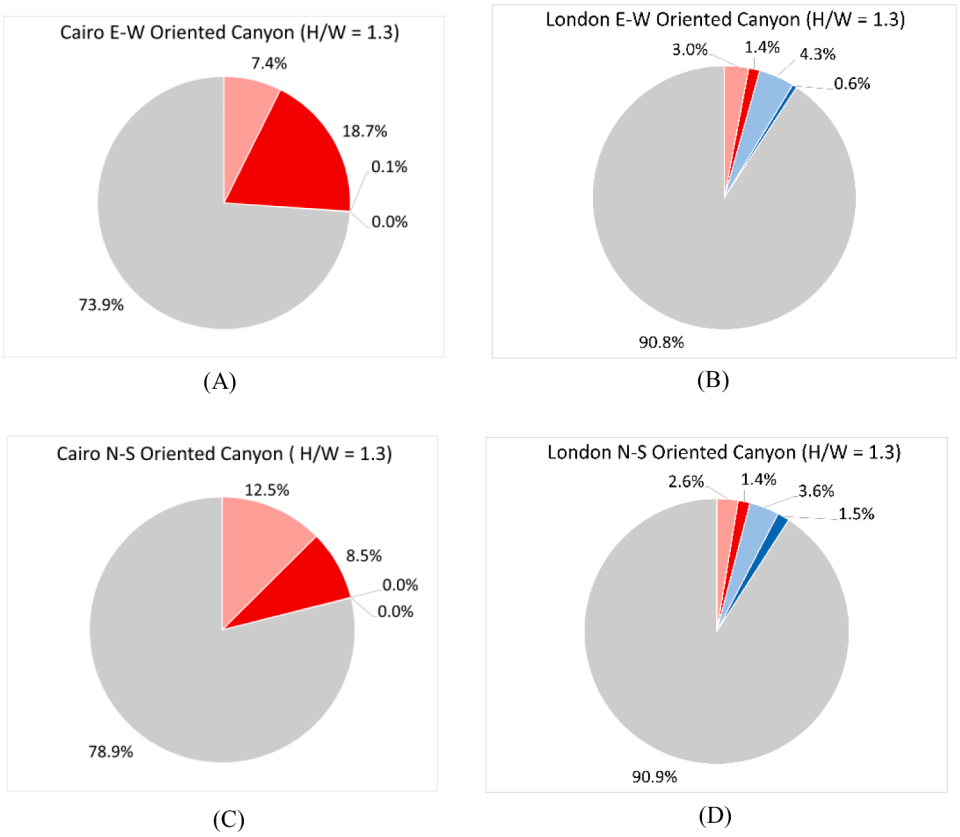

Fig. 10. The corresponding percentages of each of the 5 categories of values for the graphs shown in Fig. 9, using the same color key.

Table 4
Statistics determined from the graphs shown in Fig. 11, showing shade benefit or harm in days count.

	H/W ratio	Number of days/year where shade is highly beneficial for:			Number of days/year where shade is highly harmful for:		
		2+ Hrs.	5+ Hrs.	10+ Hrs.	2+ Hrs.	5+ Hrs.	10+ Hrs.
		E-W Oriented Canyon					
Cairo	1.3	171	164	103	0	0	0
London	1.3	26	10	0	10	0	0
		N-S Oriented Canyon					
Cairo	1.3	250	0	0	1	0	0
London	1.3	45	0	0	26	0	0
Cairo	0.9	267	159	0	0	0	0
London	0.9	55	15	0	47	0	0

more high shade harm hours for the E-W and N-S canyons for London are 10 and 26, respectively, compared to 0 and 1 for Cairo.

The outcomes of the workflow previously shown in Fig. 5 are presented for the (H/W = 0.9), for the N-S orientation for the two climates of Cairo and London, in Fig. 11. The main difference observed between the (H/W = 0.9) and the (H/W = 1.3) previously shown in Fig. 9(D & E) for Cairo and London respectively, is the expansion of the high shade benefit/harm periods over more hours of the day for the lower building heights. This is reasonable as the N-S canyon is exposed to direct solar radiation for a wider range of hours in the lower H/W ratio. The pie charts in Fig. 11(C & D), show an increase in the percentage of high shade benefit hours to 13.3% and 2.4%, for Cairo and London respectively, compared to 8.5% and 1.4% for (H/W = 1.3) previously shown in Fig. 10(C & D). While the high shade harm percentages have increased from 1.5% (H/W = 1.3) to 1.8% (H/W = 0.9) for London and remained the same (0%) for Cairo. Statistics, in Table 4, show that the number of days with 5 or more hours of high shade benefit have increased significantly in the lower H/W ratio; they increased from 0 to 159 days for Cairo, and from 0 to 15 days for London. The number of days with 2 or more hours of high shade harm have also increased in London from 26 to 47 days, while Cairo's change was insignificant.

4. Discussion

The outcome of OSAM for Cairo and London shown in the previous section highlight how results can widely vary between different climates, geometries, and orientations of urban contexts, and indicate the need for different approaches to designing the outdoor shade. Having a high percentage of high shade benefit hours, and a low percentage of shade harm over the year (like Cairo), can indicate the effectiveness of a permanent/fixed shade. However, the number of shade benefit hours per day varies between the different orientations and geometries, which are found higher in the E-W orientation of Cairo compared to the N-S (for the same H/W ratio), but also increase significantly with lower H/W ratio for the N-S canyon. Hence, further studies are needed to assess whether shade is more effective applied for the entire day, or only during the required hours, to enhance the canyon's heat release through the top during the self-shaded hours (when it is shaded by the buildings) and avoid air temperature increase. On the other hand, having some periods of high shade benefit, along with other periods of high shade harm (like London), reflects the need for temporary shades, that can be removed to allow warmth by the winter sun, or customized designs that allow the wanted sun radiations while blocking the unwanted ones based on the solar path.

Another way this method is helpful is by performing the calculations on a grid over the study space, an approximate percentage of the area that have a certain shading requirement can be known. And as the sun's position is continuously changing throughout the day, casting varying shadows across the urban context, it is useful to evaluate the shade

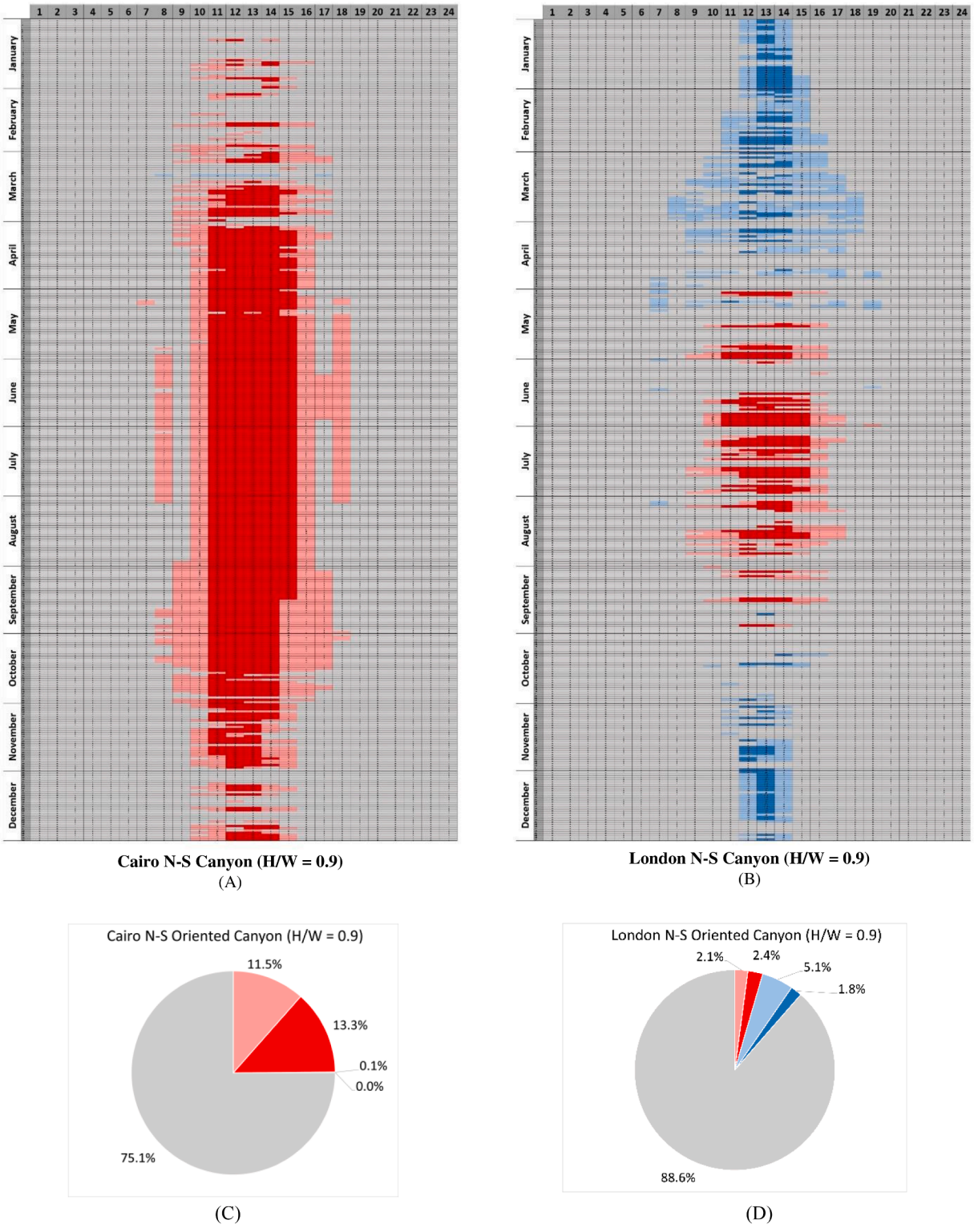

Fig. 11. Shows the repeated simulation outcome for the N-S urban canyon, with H/W ratio adjusted to be equal 0.9. The top row shows the OSAM outcome graphs for Cairo (A) and London (B) weather files. The bottom row shows the corresponding percentages for each of the 5 categories (identified previously in Fig. 9) obtained from the graphs, for Cairo (C) and London (D).

effectiveness through daily and yearly statistics, along with approximate percentages of shading-required areas. This is particularly useful for larger shade applications, which is the main target of the OSAM; like shading of a street canyon, rather than placing a small shed for a bus stop.

The LBT allowed performing large numbers of simulations, that are multiples of the 8760 hours of the year based on the number of grid points, in a few minutes time, which would otherwise not be possible. However, there are some limitations to the workflow presented. Firstly, as the method relies solely on weather data imported through the weather files (EPW files), it is important to check the reliability of the data before use, to ensure they reflect the studied space. In this study,

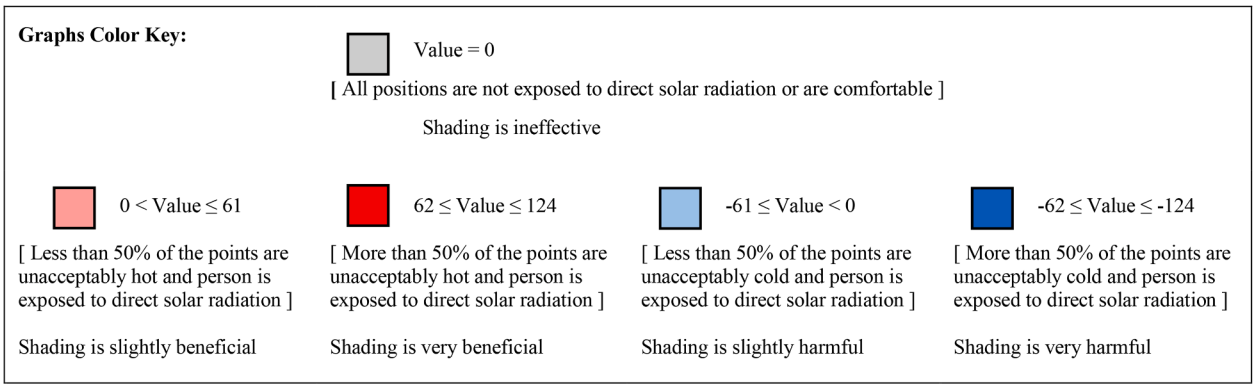

(A)

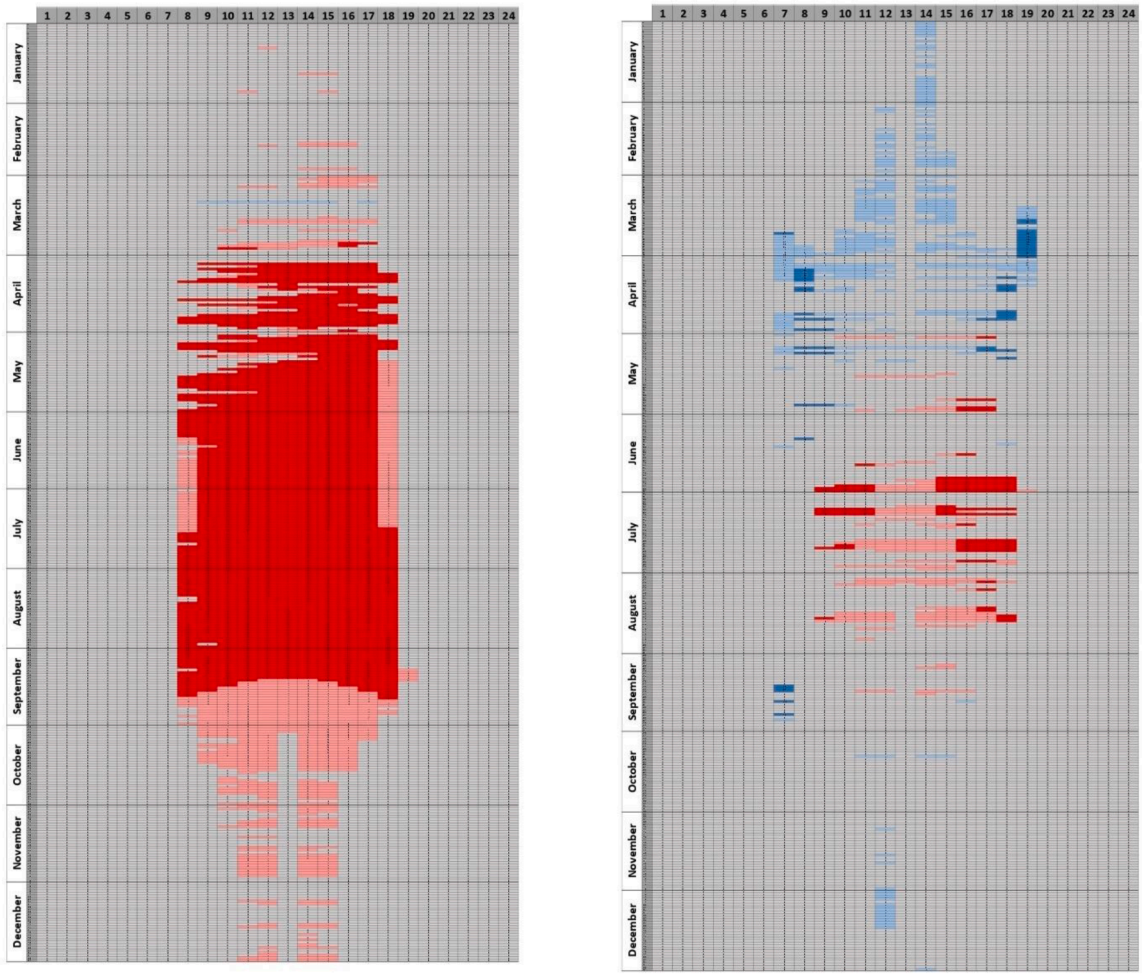

Cairo E-W Canyon

(B)

London E-W Canyon

(C)

Fig. 12. Shows the Ladybug outcome of the UTCI conditions summed up for all grid points for all the hours of the year, with the columns being the 24 h of the day, and the rows being 365 days of the year, for two different weather files. (A) shows the graph's color key. (B) and (D) show results for Cairo's International Airport Weather File, while (C) and (E) are for London Gatwick's Weather File. (B) and (C) show the results of the E-W Oriented Urban Canyon, and (D) and (E) show those of the N-S Oriented Urban Canyon.

Cairo's weather file was validated, however, London's was only provided as an example and requires validation for reliable use. Moreover, the wind simplification method used needs to be tested for open study areas and other climates; where wind speeds are higher, as it might have a bigger impact on the UTCI outcome. Furthermore, OSAM relies on the simple three-category division of comfort (hot, neutral and cold), but it does not indicate the degree of heat or cold stress that may be experienced by the pedestrians. This makes it suitable for the early analysis phase of a project to guide further in-depth studies, by pointing out statistics and identifying requirement periods, but it cannot be solely

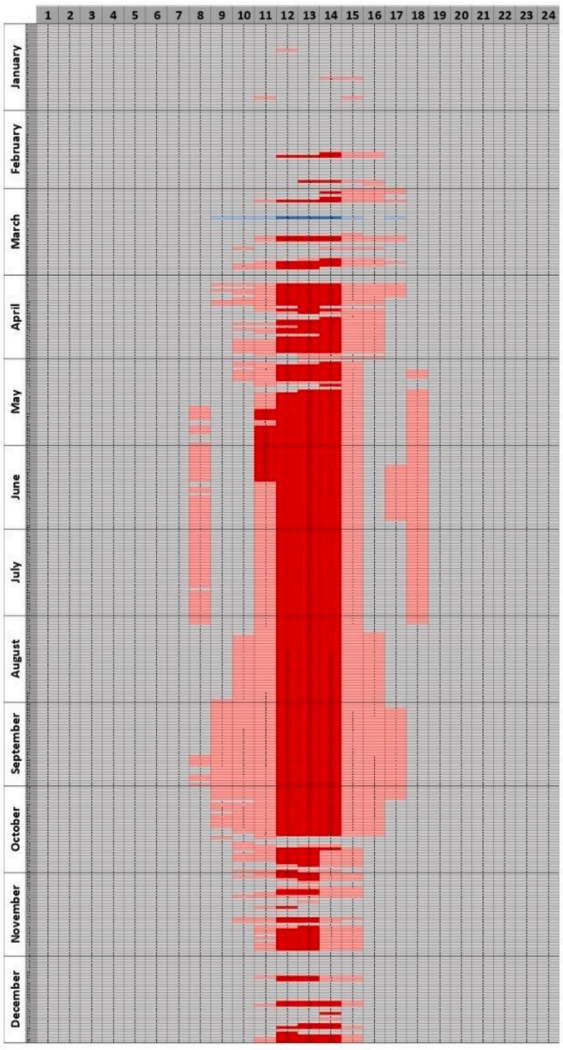

Cairo N-S Canyon

(D)

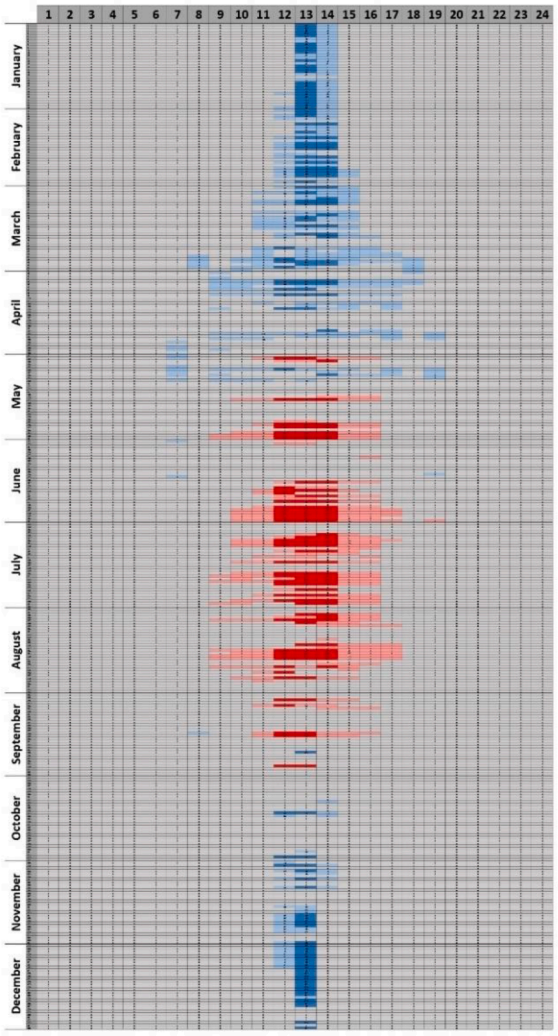

London N-S Canyon

(E)

Fig. 12. (*continued*).

relied on for the detailed analysis. In addition, the LBT software used is continuously developing and changing, with several simulation engines incorporated as plug-ins, so it requires a certain amount of knowledge to be understood and used, which practitioners may not already acknowledge.

5. Conclusions

Shading is one of the most critical strategies for enhancing the outdoor thermal environment during hot periods. However, as shading can reduce pedestrians' access to the winter sun for warmth contributing to discomfort, to ensure its effective application, it is important to analyze the potential shade benefits along with periods when shade becomes disadvantageous throughout the year. This was the aim of the new methodology presented here, the Outdoor Shading Assessment Method (OSAM).

OSAM is inspired and guided by the novel ComfortCover method, proposed by Mackey et al. (2015). It utilizes the capabilities of the new advanced software (LBT), to enhance the tools and guidance available to field practitioners on outdoor shading projects. However, unlike the use of ComfortCover, which highlights shade benefit/harm on small divisions of the proposed shade plane, OSAM provides a wider perspective on the shading requirements of a large-scale urban space for the entire year. It is intended as a simple assessment method that addresses the early analysis phase of an outdoor shade project, to guide further specific studies and shade design.

The workflow of OSAM has been tested against site-measurements in an urban canyon in Cairo. The calculations of the UTCI, which constitute the base of the methodology, obtained through the honeybee component of the LBT showed a strong correlation with those calculated from the site-measurements ($R^2 = 0.92667$) and a small difference (up to 2.22 °C), indicating reliability of the outcome. However, it also highlighted the wide gap in the MRT calculations (up to 16.63 °C) between the field measurements and the simulation software (Honeybee - LBT 1.6), specifically during the hours of direct solar exposure.

The OSAM was tested in two different climatic contexts; the hot climate of Cairo, and the temperate climate of London, for two different orientations and H/W ratios each, parallel to E-W (H/W = 1.3) and N-S (H/W = 0.9 & 1.3). The results highlighted the variations in the shading requirements throughout the year for each studied case. Cairo's contexts showed none or insignificant harm done by shading throughout the year, unlike London, that showed some periods where shade can be harmful. Moreover, Cairo's N-S canyon showed more days requiring shade for at least 2 hours, compared to the E-W canyon for the same H/

W ratio, however, the latter showed longer shade requirement hours per day (5+ hours). In addition, the number of days with high shade benefit for 5 or more hours have increased significantly in Cairo (from 0 to 159 days), as the H/W ratio for the N-S canyon was lowered from 1.3 to 0.9.

OSAM demonstrates how the advanced capabilities of the simulation tools (LBT) can be utilized for the analysis of outdoor environments in terms of shading requirements. Its outcome constitutes a base that guides further specific analytical studies; such as studies on the micro-climate, outdoor surface temperatures, solar radiation intensity, and others by targeting specific identified periods of shade benefit/harm. Moreover, the graphical presentation used in OSAM can be adopted in future environmental studies that involve numerous numerical data; to simplify the process of analyzing the outcome and facilitate comparisons between different scenarios (e.g. impact of different shade designs). In addition, OSAM and other future dependent studies supported by simulations, may play a role in the development of outdoor shading policies and guidelines, supporting the implementation of large-scale shades, the expansion of urban areas, and the pedestrianization and/or development of existing urban contexts, through enhanced outdoor thermal comfort by shading.

Declaration of Competing Interest

The authors declare that they have no known competing financial interests or personal relationships that could have appeared to influence the work reported in this paper.

Data availability

Data will be made available on request.

Acknowledgements

We sincerely thank Dr. Yasser Ibrahim from University of Bath, UK, and Dr. Ibrahim Elwy from Military Technical College, Egypt, for providing us with Cairo's field measurements data, that we used to compare to our simulation workflow outcome for the validation of the study.

This work has been funded by a full scholarship [MM16/21] from the Ministry of Higher Education of the Arab Republic of Egypt.

Appendix

OSAM outcome using the ladybug components workflow for (H/W = 1.3).

References

Abbasi, A., Alalouch, C., & Bramley, G. (2016). Open space quality in deprived urban areas: User perspective and use pattern. *Procedia - Social and Behavioral Sciences, 216*, 194–205.

Ali-Toudert, F., & Mayer, H. (2006). Numerical study on the effects of aspect ratio and orientation of an urban street canyon on outdoor thermal comfort in hot and dry climate. *Building and Environment, 41*, 94–108.

Andreou, E. (2014). The effect of urban layout, street geometry and orientation on shading conditions in urban canyons in the Mediterranean. *Renewable Energy, 63*, 587–596.

ANSI/ASHRAE Standard 55-2004. (2004). *Thermal environmental conditions for human occupancy*. ASHRAE.

ASHRAE. (2001). *International weather for energy calculations (IWEC weather files) users manual and cd-rom*. Atlanta.

ASHRAE. (2005). Chapter 16: Airflow around buildings. *Handbook - Fundamentals (SI)*. American Society of Heating Refrigerating and Air Conditioning Engineers.

Aynsley, R. M., Melbourne, W., & Vickery, B. J. (1977). *Architectural aerodynamics*. Applied Science Publishers.

Błażejczyk, K., Broede, P., Fiala, D., Havenith, G., Holmér, I., Jendritzky, G., … Kunert, A. (2010). Principles of the new universal thermal climate index (UTCI) and its application to bioclimatic research in european scale. *Miscellanea Geographica, 14* (1), 91–102.

Blazejczyk, K., Epstein, Y., Jendritzky, G., Staiger, H., & Tinz, B. (2012). Comparison of UTCI to selected thermal indices. *International Journal of Biometeorology, 56*, 515–535.

British Standards Institution, Ergonomics of the thermal environment. (2001). *Instruments for measuring physical quantities*. BSI.

Chung, D. H. J., & Choo, M.-L. L. (2011). Computational fluid dynamics for urban design: The prospects for greater integration. *International Journal of Architecture Computing, 9*(1), 33–53.

Copernicus Climate Change Service (C3S), "Thermal Comfort Indices - Universal Thermal Climate Index, 1979-2020," [Online]. Available: https://climate-adapt.eea.europa.eu/metadata/indicators/thermal-comfort-indices-universal-thermal-climate-index-1979-2019 [Accessed 30 06 2022].

DOE, "Weather Data," (2023). [Online]. Available: https://energyplus.net/weather [Accessed 20 01 2023].

Elliott, H., Eon, C., & Breadsell, J. K. (2020). Improving city vitality through urban heat reduction with green infrastructure and design solutions: A systematic literature review. *Buildings, 10*(12), 219.

Eltaweel, A., Su, Y., Lv, Q., & Lv, H. (2020). Advanced parametric louver systems with bi-axis and two layer designs for an extensive daylighting coverage in a deep-plan office room. *Solar Energy, 206*, 596–613.

Elwy, I., & Ibrahim, Y. (2022). Urban canyon outdoor microclimate field measurements in Cairo, Egypt. *Mendeley Data*.

Evola, G., Costanzo, V., Magrì, C., & Margani, G. (2020). A novel comprehensive workflow for modelling outdoor thermal comfort and energy demand in urban canyons: Results and critical issues. *Energy and Buildings, 216*, Article 109946.

Fang, Z., Feng, X., & Lin, Z. (2017). Investigation of PMV model for evaluation of the outdoor thermal comfort. *Procedia Engineering, 205*, 2457–2462.

Garcia-Nevado, E., Beckers, B., & Coch, H. (2020). Assessing the cooling effect of urban textile shading devices through time-lapse thermography. *Sustainable Cities and Society, 63*, 102458.

Givoni, B., Noguchi, M., Saaroni, H., Pochter, O., Yaacov, Y., Feller, N., & Becker, S. (2003). Outdoor comfort research issues. *Energy and Buildings, 35*, 77–86.

Google Earth, Airbus, (2023).

Ibrahim, Y., Kershaw, T., Shepherd, P., & Elwy, I. (2021). A parametric optimisation study of urban geometry design to assess outdoor thermal comfort. *Sustainable Cities and Society, 75*, 103352.

Ibrahim, Y. I., Kershaw, T., & Shepherd, P. (2020). A methodology for modelling microclimate: A Ladybug-tools and ENVI-met verification study. In *35th Plea Conference Sustainable Architecture And Urban Design: Planning Post Carbon Cities, A Coruña*.

Kong, L., Lau, K. K.-L., Yuan, C., Chen, Y., Xu, Y., Ren, C., & Ng, E. (2017). Regulation of outdoor thermal comfort by trees in Hong Kong. *Sustainable Cities and Society, 31*, 12–25.

Lai, D., Zhou, C., Huang, J., Jiang, Y., Long, Z., & Chen, Q. (2014). Outdoor space quality: A field study in an urban residential community in central China. *Energy and Buildings, 68*(part B), 713–720.

Lam, C. K. C., Hang, J., Zhang, D., Wang, Q., & Ren, M. (2021). Effects of short-term physiological and psychological adaptation on summer thermal comfort of outdoor exercising people in China. *Building and Environment, 198*, 107877.

Li, K., Liu, X., & Bao, Y. (2022). Evaluating the performance of different thermal indices on quantifying outdoor thermal sensation in humid subtropical residential areas of China. *Frontiers in Environmental Science, 10*, 1071668.

Lin, H., Ni, H., Xiao, Y., & Zhu, X. (2023). Couple simulations with CFD and ladybug + honeybee tools for green facade optimizing the thermal comfort in a transitional space in hot-humid climate. *Journal of Asian Architecture and Building Engineering, 22*, 1317–1342.

Lin, T.-P., Matzarakis, A., & Hwang, R.-L. (2010). Shading effect on long-term outdoor thermal comfort. *Building and Environment, 45*, 213–221.

Mackey, C., Roudsari, M. S., & Samaras, P. (2015). ComfortCover: A novel method for the design of outdoor shades. In *SimAUD '15: Proceedings of the Symposium on Simulation for Architecture & Urban Design, Alexandria, Virginia*.

Mahgoub, M. H. K. E. (2015). *Assessment of thermal comfort and visual micro-climate of a traditional commercial street in a hot arid climate*. Newcastle: Newcastle University.

Matzarakis, A., Martinelli, L., & Ketterer, C. (2016). Chapter 4: Revelance of thermal indices for the assessment of the urban heat island. In F. Musco (Ed.), *Counteracting urban heat island effect in a global climate change scenario* (pp. 93–107). Springer Nature.

Matzarakis, A., Muthers, S., & Rutz, F. (2014). Application and comparison of UTCI and PET in temperate climate conditions. *Finisterra - Revista Portuguesa de Geografia, 49*, 21–31.

Middel, A., Selover, N., Hagen, B., & Chhetri, N. (2016). Impact of shade on outdoor thermal comfort - a seasonal field study in Tempe, Arizona. *International Journal of Biometeorology, 60*, 1849–1861.

Naboni, E., Meloni, M., Mackey, C., & Kaempf, J. (2019). The simulation of mean radiant temperature in outdoor conditions: A review of software tools capabilities. In *16th IBPSA International Conference and Exhibition, Rome*.

Nasution, A. D., & Zahrah, W. (2018). Quality of life: Public open space effects. *Asian Journal of Environment-Behaviour Studies, 3*, 124–132.

Natanian, J., Kastner, P., Dogan, T., & Auer, T. (2020). From energy performative to livable Mediterranean cities: An annual outdoor thermal comfort and energy balance cross-climatic typological study. *Energy and Buildings, 224*, 110283.

Nikolopoulou, M. (2011). Outdoor thermal comfort. *Frontiers in Bioscience-Scholar (FBS), 3*(4), 1552–1568.

Nikolopoulou, M. (2021). Chapter 4: Thermal comfort in urban spaces. In M. Palme, & A. Salvati (Eds.), *Urban microclimate modelling for comfort and energy studies* (pp. 55–77). eBook, Springer Nature Switzerland AG.

Nikolopoulou, M., Baker, N., & Steemers, K. (2001). Thermal comfort in outdoor urban spaces: Understanding the human parameter. *Solar Energy, 70*, 227–235.
Nikolopoulou, M., & Lykoudis, S. (2007). Use of outdoor spaces and microclimate in a Mediterranean urban area. *Building and Environment, 42*, 3691–3707.
Nikolopoulou, M., & Steemers, K. (2003). Thermal comfort and psychological adaptation as a guide for designing urban spaces. *Energy and Buildings, 35*, 95–101.
Oke, T. R. (1988). Street design and urban canopy layer climate. *Energy and Buildings, 11*, 103–113.
Jänicke, B., Meier, F., Hoelscher, M., & Scherer, D. (2015). Evaluating the effects of facade greening on human bioclimate in a complex urban environment. Advances in Meteorology, 2015, 747259.
Nasir, R.A., Ahmad, S.S., & Ahmed, A.Z. (2012). Psychological adaptation of outdoor thermal comfort in shaded green spaces in Malaysia. AicE-Bs 2012 Cairo, 68, 865-878.
Oke, T.R. (1995). The heat island of the urban boundary layer: characteristics, causes and effects, in *Wind climate in cities*, Vols. NATO ASI Series, 277, J.E. Cermak, A.G. Davenport, E.J. Plate and D.X. Viegas, Eds., Springer, pp. 81–107.
Pacifici, M., & Nieto-Tolosa, M. (2021). Chapter 14: Comparing ENVI-Met and grasshopper modelling strategies to assess local thermal stress and urban heat island effects. In A. S. Massimo Palme (Ed.), *Urban microclimate modelling for comfort and energy studies* (pp. 293–316). Springer.
Pantavou, K., Theoharatos, G., Santamouris, M., & Asimakopoulos, D. (2013). Outdoor thermal sensation of pedestrians in a Mediterranean climate and a comparison with UTCI. *Building and Environment, 66*, 82–95.
Peeters, A., Shashua-Bar, L., Meir, S., Shmulevich, R. R., Caspi, Y., Weyl, M., … Angel, N. (2020). A decision support tool for calculating effective shading in urban Streets. *Urban Climate, 34*, 100672.
Potchter, O., Cohen, P., Lin, T.-P., & Matzarakis, A. (2018). Outdoor human thermal perception in various climates: A comprehensive review of approaches, methods and quantification. *Science of The Total Environment, 631-632*, 390–406.
Radiance, "Setting Rendering Options," The university of California, [Online]. Available: https://radsite.lbl.gov/radiance/refer/Notes/rpict_options.html. [Accessed 10 05 2023].
Roudsari, M. S., & Pak, M. (2013). Ladybug: A parametric environmental plugin for grasshopper to help designers create an environmentally-conscious design. In *13th International Conference of Building Performance Simulation Association, Chambery, France*.
Setaih, K., Hamza, N., Mohammed, M. A., Dudek, S., & Townshend, T. (2014). CFD modeling as a tool for assessing outdoor thermal comfort conditions in urban settings in hot arid climates. *Journal of Information Technology in Construction, 19*, 248–269.
Staiger, H., Laschewski, G., & Matzarakis, A. (2019). Selection of appropriate thermal indices for applications in human biometeorological studies. *Atmosphere, 10*(1), 18.
Tahbaz, M. (2016). Estimation of the wind speed in urban areas - Height less than 10 metres. *International Journal of Ventilation, 8*, 75–84.
The Central Agency for Public Mobilization and Statistics in Cairo, Cairo, (2022).
Vanos, J. K., Warland, J. S., Gillespie, T. J., & Kenny, N. A. (2010). Review of the physiology of human thermal comfort while exercising in urban landscapes and implications for bioclimatic design. *International Journal of Biometeorology, 54*, 319–334.
Wang, C., Wang, Z.-H., & Yang, J. (2018). Cooling Effect of Urban Trees on the Built Environment of Contaguous United States. *Earth's Future, 6*, 1066–1081.
Xu, X., Wu, Y., Wang, W., Hong, T., & Xu, N. (2019). Performance-driven optimization of urban open space configuration in the cold-winter and hot-summer region of China. *Building Simulation, 12*, 411–424.
Zhao, Q., Lian, Z., & Lai, D. (2021). Thermal comfort models and their developments: A review. *Energy and Built Environment, 2*(1), 21–33.